V.N. Baier and V.M. Katkov

SPECTRA OF RADIATION
AND CREATED PARTICLES
AT INTERMEDIATE ENERGY
IN ORIENTED CRYSTAL
TAKING INTO ACCOUNT ENERGY LOSS

Spectra of radiation and created particles at intermediate energy in oriented crystal taking into account energy loss

V.N. Baier and V.M. Katkov

Institute of Nuclear Physics
630090, Novosibirsk, Russia

Abstract

The spectral distribution of positron created by photon and the spectral distribution of photons radiated from electron in an oriented single crystal of intermediate thickness is calculated at intermediate energies. The energy loss of charged particles as well as photon absorption are taken into account. The used basic probabilities of processes include the action of field of axis as well as the multiple scattering of radiating electron or particles of the created pair (the Landau-Pomeranchuk-Migdal (LPM) effect).

1 Introduction

1. In crystals oriented along main axes the probabilities of photon emission from an electron and e^+e^- pair creation by a photon are strongly enhanced comparing to the corresponding amorphous media. The example is shown in Fig.1, where the crystal radiation length $L(\varepsilon) = \varepsilon/I(\varepsilon)$, $I(\varepsilon)$ is the intensity of electron radiation, and the pair creation length $L_{pr}(\omega) = 1/W(\omega)$, $W(\omega)$ is the pair creation probability, are plotted as a function of the corresponding energy. The both functions $I(\varepsilon)$ and $W(\omega)$ are calculated in frame of the new method, developed recently by authors [1, 2], which permits inseparable consideration of both coherent and incoherent mechanisms of the process.
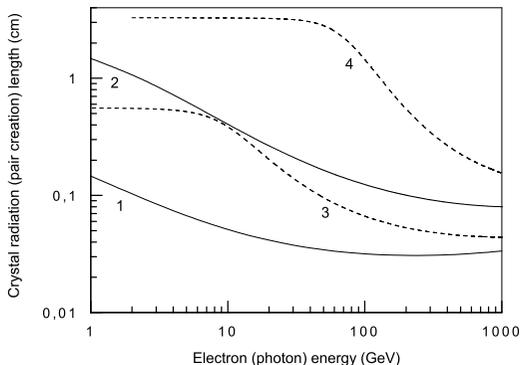

Fig. 1. The radiation length $L(\varepsilon) = \varepsilon/I(\varepsilon)$ (curve 1)and the pair creation length $L_{pr}(\omega) = 1/W(\omega)$ (curves 3) in the tungsten crystal, axis $< 111 >$, temperatures T=100 K. The values $L(\varepsilon)$ (curve 2) and $L_{pr}(\omega)$ (curve 4) in the germanium crystal, axis $< 110 >$, temperatures T=293 K vs the electron (ε) or photon (ω) energy.

It is seen that there are two regions of $L_{pr}(\omega)$. In the first one $L_{pr}(\omega)$ is almost constant. This is the incoherent contribution (or, in other words, the Bethe-Maximon contribution with the crystal corrections). It is seen that in this region $L \ll L_{pr}$, what means that the probability of pair creation pro-

3

TABLE Parameters of the pair photoproduction and radiation processes in the tungsten crystal, axis $< 111 >$ and the germanium crystal, axis $< 110 >$ for two temperatures T $(\varepsilon_0 = \omega_0/4, \varepsilon_m = \omega_m, \varepsilon_s = \omega_s)$

Crystal	T(K)	V_0(eV)	x_0	η_1	η	ω_0(GeV)	ε_m(GeV)	ε_s(GeV)	h
W	293	417	39.7	0.108	0.115	29.7	14.35	34.8	0.348
W	100	355	35.7	0.0401	0.0313	12.25	8.10	43.1	0.612
Ge	293	110	15.5	0.125	0.119	592	88.4	210	0.235
Ge	100	114.5	19.8	0.064	0.0633	236	50.5	179	0.459

cess is still close to the probability in the corresponding amorphous medium while the radiation length $L(\varepsilon)$ (connected with the electron energy loss) is strongly enhanced (mostly due to the soft photons emission) comparing with the corresponding amorphous medium and the energy loss of electrons and positrons is strongly influenced on the processes. This is true in the first region where to one can add the vicinity of the turn point of the function $L_{pr}(\omega)$ at $\omega \simeq \omega_m \equiv \varepsilon_m$ (see Table) where $L(\varepsilon_m)W(\omega_m) \ll 1$, e.g. in tungsten at $\varepsilon = 20$ GeV $L_{pr} \simeq 4.9L$ and in germanium at $\varepsilon = 200$ GeV $L_{pr} \simeq 5.5L$. In this (intermediate) electron and photon energy region it is impossible to separate the coherent and incoherent contributions to the probability of basic processes. In particular, one can't represent the probability as the sum of contribution in the crystal field and the Bethe-Maximon contribution. This is because one has to include action of the crystal field on the incoherent process as well as the multiple scattering of emitting electron or particles of created pair for the process in field. These items were discussed in the authors recent paper [3].

2. Basing on Eqs.(16) and (17) of [1] (see also Eq.(7.135) in [5]) one get the general expression for the spectral distribution of particles created by a photon

$$dW(\omega, y) = \frac{\alpha m^2}{2\pi\omega} \frac{dy}{y(1-y)} \int\limits_0^{x_0} \frac{dx}{x_0} G(x,y), \quad G(x,y) = \int\limits_0^\infty F(x,y,t)dt + s_3\frac{\pi}{4},$$

$$F(x,y,t) = \mathrm{Im}\left\{ e^{f_1(t)}\left[s_2\nu_0^2(1+ib)f_2(t) - s_3 f_3(t) \right] \right\}, \quad b = \frac{4\kappa_1^2}{\nu_0^2}, \quad y = \frac{\varepsilon}{\omega},$$

$$f_1(t) = (i-1)t + b(1+i)(f_2(t) - t), \quad f_2(t) = \frac{\sqrt{2}}{\nu_0}\tanh\frac{\nu_0 t}{\sqrt{2}},$$

$$f_3(t) = \frac{\sqrt{2}\nu_0}{\sinh(\sqrt{2}\nu_0 t)}, \tag{1}$$

4

where

$$s_2 = y^2 + (1-y)^2, \ \ s_3 = 2y(1-y), \ \ \nu_0^2 = 4y(1-y)\frac{\omega}{\omega_c(x)}, \ \ \kappa_1 = y(1-y)\kappa(x), \tag{2}$$

ε is the energy of one of the created particles.

The situation is considered when the photon angle of incidence ϑ_0 (the angle between photon momentum $\mathbf{k}$ and the axis) is small under condition $\vartheta_0 \ll V_0/m$. The axis potential (see Eq.(9.13) in [5]) is taken in the form

$$U(x) = V_0 \left[\ln \left(1 + \frac{1}{x+\eta} \right) - \ln \left(1 + \frac{1}{x_0 + \eta} \right) \right], \tag{3}$$

where

$$x_0 = \frac{1}{\pi d n_a a_s^2}, \quad \eta_1 = \frac{2u_1^2}{a_s^2}, \quad x = \frac{\varrho^2}{a_s^2}, \tag{4}$$

Here ϱ is the distance from axis, u_1 is the amplitude of thermal vibration, d is the mean distance between atoms forming the axis, a_s is the effective screening radius of the potential. The parameters in Eq.(3) were determined by means of fitting procedure, see Table.

The local value of parameter $\kappa(x)$ which determines the probability of pair creation in the field Eq.(3) is

$$\kappa(x) = -\frac{dU(\varrho)}{d\varrho}\frac{\omega}{m^3} = 2\kappa_s f(x), \ f(x) = \frac{\sqrt{x}}{(x+\eta)(x+\eta+1)}, \ \kappa_s = \frac{V_0\omega}{m^3 a_s} \equiv \frac{\omega}{\omega_s}. \tag{5}$$

For an axial orientation of crystal the ratio of the atom density $n(\varrho)$ in the vicinity of an axis to the mean atom density n_a is (see [1])

$$\frac{n(x)}{n_a} = \xi(x) = \frac{x_0}{\eta_1}e^{-x/\eta_1}, \quad \omega_0 = \frac{\omega_e}{\xi(0)}, \quad \omega_e = 4\varepsilon_e = \frac{m}{4\pi Z^2 \alpha^2 \lambda_c^3 n_a L_0}. \tag{6}$$

The functions and values in Eqs.(1) and (2) are

$$\omega_c(x) = \frac{\omega_e(n_a)}{\xi(x)g_p(x)} = \frac{\omega_0}{g_p(x)}e^{x/\eta_1}, \quad g_{p0} = 1 - \frac{1}{L_0}\left[\frac{1}{42} + h\left(\frac{u_1^2}{a^2}\right)\right],$$

$$g_p(x) = g_{p0} + \frac{1}{6L_0}\left[\ln\left(1+\kappa_1^2\right) + \frac{6D_p\kappa_1^2}{12+\kappa_1^2}\right],$$

$$h(z) = -\frac{1}{2}\left[1 + (1+z)e^z \mathrm{Ei}(-z)\right], \quad L_0 = \ln(ma) + \frac{1}{2} - f(Z\alpha),$$

$$a = \frac{111Z^{-1/3}}{m}, \quad f(\xi) = \sum_{n=1}^{\infty} \frac{\xi^2}{n(n^2+\xi^2)}, \tag{7}$$

5

where where Z is the charge of nucleus, $f(\xi)$ is the Coulomb correction, the function $g_p(x)$ determines the effective logarithm using the interpolation procedure, $D_p = D_{sc} - 10/21 = 1.8246$, $D_{sc} = 2.3008$ is the constant entering in the radiation spectrum at $\chi/u \gg 1$ (or in electron spectrum in pair creation process at $\kappa_1 \gg 1$), see Eq.(7.107) in [5], $\text{Ei}(z)$ is the integral exponential function.

The expression for $dW(\omega, y)$ Eq.(1) includes both the coherent and incoherent contributions as well as the influence of the multiple scattering (the LPM effect) on the pair creation process (see [1]).

3. The expression for the spectral probability of radiation used in the above derivation can be found from the spectral distribution Eq.(1) $(dW/dy = \omega dW/d\varepsilon)$ using the standard QED substitution rules: $\varepsilon \to -\varepsilon$, $\omega \to -\omega$, $\varepsilon^2 d\varepsilon \to \omega^2 d\omega$ and exchange $\omega_c(x) \to 4\varepsilon_c(x)$. As a result one has for the spectral intensity $dI = \omega dW$

$$dI(\varepsilon, y_r) = \frac{\alpha m^2}{2\pi} \frac{y_r dy_r}{1 - y_r} \int\limits_0^{x_0} \frac{dx}{x_0} G_r(x, y_r),$$

$$G_r(x, y_r) = \int\limits_0^\infty F_r(x, y_r, t)dt - r_3\frac{\pi}{4},$$

$$F_r(x, y_r, t) = \text{Im}\left\{ e^{\varphi_1(t)} \left[r_2\nu_{0r}^2(1 + ib_r)f_2(t) + r_3 f_3(t) \right] \right\}, \quad b_r = \frac{4\chi^2(x)}{u^2\nu_{0r}^2},$$

$$y_r = \frac{\omega}{\varepsilon}, \quad u = \frac{y_r}{1 - y_r}, \quad \varphi_1(t) = (i-1)t + b_r(1+i)(f_2(t) - t), \quad (8)$$

where

$$r_2 = 1 + (1 - y_r)^2, \quad r_3 = 2(1 - y_r),$$
$$\nu_{0r}^2 = \frac{1 - y_r}{y_r} \frac{\varepsilon}{\varepsilon_c(x)}, \quad (9)$$

where the functions $f_2(t)$ and $f_3(t)$ are defined in Eq.(1). The local value of parameter $\chi(x)$ which determines the radiation probability in the field Eq.(3) is

$$\chi(x) = -\frac{dU(\varrho)}{d\varrho} \frac{\varepsilon}{m^3} = 2\chi_s f(x), \quad \chi_s = \frac{V_0\varepsilon}{m^3 a_s} \equiv \frac{\varepsilon}{\varepsilon_s}, \quad (10)$$

where $f(x)$ is defined in Eq.(5).

6

The functions and values in Eqs.(8) and (9) (see also Eqs.(6) and (7)) are

$$\varepsilon_c(x) = \frac{\varepsilon_e(n_a)}{\xi(x)g_r(x)} = \frac{\varepsilon_0}{g_r(x)}e^{x/\eta_1},$$

$$g_r(x) = g_{r0} + \frac{1}{6L_0}\left[\ln\left(1 + \frac{\chi^2(x)}{u^2}\right) + \frac{6D_r\chi^2(x)}{12u^2 + \chi^2(x)}\right],$$

$$g_{r0} = 1 + \frac{1}{L_0}\left[\frac{1}{18} - h\left(\frac{u_1^2}{a^2}\right)\right], \tag{11}$$

where the function $g_r(x)$ determines the effective logarithm using the interpolation procedure: $D_r = D_{sc} - 5/9 = 1.7452$.

The expression for dI Eq.(8) includes both the coherent and incoherent contributions as well as the influence of the multiple scattering (the LPM effect) on the photon emission process (see [2]).

2 Inclusion of energy loss and photon absorption

Here we consider the processes of interaction of electrons and photons with oriented crystal when the target thickness l is of the order $l \sim L(\varepsilon)$ in the intermediate energy region.

Below we will neglect the energy dispersion (see discussion in Sec.17.5 [5]). On this assumption the energy loss equation acquires the form

$$dt = \frac{L(\varepsilon)}{\varepsilon}d\varepsilon, \quad t(\varepsilon, \varepsilon_0) = \int_\varepsilon^{\varepsilon_0} \frac{dx}{x}L(x), \quad \varepsilon = \varepsilon(\varepsilon_0, t) \tag{12}$$

Now the photon spectral distribution taking into account the energy loss can be written in the form (cp Eq.(20.36) [5] for the total number of photons)

$$\omega\frac{dn_\gamma^{(in)}}{d\omega} = \int_0^l \frac{dI(\varepsilon(\varepsilon_0, t), \omega)}{d\omega}\vartheta(\varepsilon(\varepsilon_0, t) - \omega)dt$$

$$= \int_{\varepsilon_l}^{\varepsilon_0} \frac{L(\varepsilon)}{\varepsilon}\frac{dI(\varepsilon, \omega)}{d\omega}\vartheta(\varepsilon - \omega)d\varepsilon, \quad \varepsilon_l = \varepsilon(\varepsilon_0, l), \tag{13}$$

where $dI(\varepsilon, \omega)/d\omega$ is radiation intensity spectral distribution (see Eq.(8)).

7

For calculation of the photon spectral distribution at the exit from a target one has to take into account the photon absorption on the length $l - t$. This can be done by substitution the additional factor $\exp(-W(\omega)(l-t))$ into the integrand of Eq.(13):

$$\frac{dn_\gamma^{(out)}}{d\omega} = \frac{1}{\omega} \int_0^l \exp(-W(\omega)(l-t)) \frac{dI(\varepsilon(\varepsilon_0, t), \omega)}{d\omega} \vartheta(\varepsilon(\varepsilon_0, t) - \omega) dt$$

$$= \frac{\exp(-W(\omega)l)}{\omega} \int_{\varepsilon_l}^{\varepsilon_0} \frac{L(\varepsilon)}{\varepsilon} \exp(W(\omega)t(\varepsilon, \varepsilon_0)) \frac{dI(\varepsilon, \omega)}{d\omega} \vartheta(\varepsilon - \omega) d\varepsilon, \quad (14)$$

where $W(\omega)$ is the probability of pair creation by a photon with the energy ω per unit time.

In the case $\omega > \varepsilon_l$ the lower limit of the integrals in Eqs.(13),(14) becomes ω because of the function $\vartheta(\varepsilon - \omega)$ in the integrand. In this case, the integral in Eq.(13) dos't depend on the target thickness, while the spectral distribution in Eq.(14) contains the target thickness in the common factor $\exp(-W(\omega)l)$ only. The difference of the number of the emitted photon and the number of outgoing photons gives the number of the created pairs: $n_p = n_\gamma^{(in)} - n_\gamma^{(out)}$.

We consider now the hard end ($\varepsilon_0 - \omega \ll \varepsilon_0$, $t(\omega, \varepsilon_0) \ll l$) of the spectral distribution in Eq.(14), where the radiation spectral intensity is defined by the incoherent contribution only ($\varepsilon_0 - \omega \ll 2\varepsilon_m/3$). In this situation one has

$$\frac{dn_\gamma^{(out)}}{d\omega} \simeq \frac{L(\varepsilon_0)g_{r0}}{L_{rad}} \exp(-W(\varepsilon_0)l) \frac{\varepsilon_0 - \omega}{\varepsilon_0^2} \quad (15)$$

For soft photons the spectral intensity of radiation depends rather weakly on the radiating electron energy (see e.g. Fig.3a in [3]). Than using the first equality in Eq.(13) we get

$$\frac{dn_\gamma^{(in)}}{d\omega} \simeq \frac{l}{\omega} \frac{dI(\varepsilon_0, \omega)}{d\omega} \quad (16)$$

One can found more accurate expression using the second equality in Eq.(13) and caring out the averaging procedure given in [2] (see Eqs.(20)-(24)):

$$\frac{dn_\gamma^{(in)}}{d\omega} = \frac{l}{\omega} \frac{d\tilde{I}}{d\omega}, \quad \frac{d\tilde{I}}{d\omega} = \frac{\tilde{\varepsilon}L(\varepsilon_0)\frac{dI(\varepsilon_0, \omega)}{d\omega} + \varepsilon_0 L(\tilde{\varepsilon})\frac{dI(\tilde{\varepsilon}, \omega)}{d\omega}}{\tilde{\varepsilon}L(\varepsilon_0) + \varepsilon_0 L(\tilde{\varepsilon})}, \quad (17)$$

$$\tilde{\varepsilon} = \varepsilon_0 \exp\left(-\frac{l}{\tilde{L}}\right), \quad \tilde{L} = \frac{\varepsilon_0 L(\varepsilon_1) + \varepsilon_1 L(\varepsilon_0)}{\varepsilon_1 + \varepsilon_0}, \quad \varepsilon_1 = \varepsilon_0 \exp\left(-\frac{l}{L(\varepsilon_0)}\right).$$

8

The probability of soft photons absorption is determined by the incoherent contribution of pair creation $W(\omega) \simeq 7g_{p0}/9L_{rad}$, where L_{rad} is the radiation length in a corresponding amorphous medium, and is small for the target thickness under consideration $l \sim L \ll L_{rad}$. In this case using the difference of the first equalities in Eq.(13) and Eq.(14) we find for the spectral distribution of created pairs $\omega = \varepsilon^+ + \varepsilon^-$

$$\frac{dn_\gamma^{(in)}}{d\omega} \simeq \frac{l^2}{2\omega} \frac{dI(\varepsilon_0, \omega)}{d\omega} W(\omega) \tag{18}$$

In the process of pair photoproduction the spectral distribution of created particles changes due to the radiation energy loss before leaving a target. Let us introduce the integral with δ-function into the initial distribution. We have at the distance t before leaving a target

$$dw(\varepsilon, \varepsilon', t) = -\frac{dW(\omega, \varepsilon')}{d\varepsilon'} \exp(-W(\omega)(l-t))\delta(t(\varepsilon, \varepsilon') - t)\frac{dt(\varepsilon, \varepsilon')}{d\varepsilon} d\varepsilon d\varepsilon' dt, \tag{19}$$

where $dW(\omega, \varepsilon')/d\varepsilon'$ is the spectral distribution over energy of one of the created particles in the point of creation (see Eq.(1)) at the distance t before leaving a target, the function $t(\varepsilon, \varepsilon')$ is defined in Eq.(12)). The factor $\exp(-W(\omega)(l-t))$ is the probability of the initial photon to survive at the depth $l - t$. Caring out the integration in Eq.(19)) over variables ε' and t we get

$$\frac{dw(\omega, \varepsilon)}{d\varepsilon} = \frac{L(\varepsilon)}{\varepsilon} \exp(-W(\omega)l) \int_\varepsilon^{\varepsilon_p} \frac{dW(\omega, \varepsilon')}{d\varepsilon'} \exp(W(\omega)t(\varepsilon, \varepsilon'))\vartheta(\omega - \varepsilon')d\varepsilon', \tag{20}$$

In the case $\omega < \varepsilon_p$ the upper limit of the integral in Eq.(20) becomes ω because of the function $\vartheta(\omega - \varepsilon')$ in the integrand. In this case, the integral in Eq.(20) dos't depend on the target thickness, which enters in the external factor $\exp(-W(\omega)l)$ only.

Let us consider the hard end $(\omega - \varepsilon \ll \omega,\ t(\varepsilon, \varepsilon') \ll l)$ of the spectral distribution in Eq.(20), where the spectral probability of pair creation is defined by the incoherent contribution only $(\omega - \varepsilon \ll 2\omega_m/3)$. In this situation one has

$$\frac{dw(\omega, \varepsilon)}{d\varepsilon} \simeq \frac{L(\omega)g_{p0}}{L_{rad}} \exp(-W(\omega)l)\frac{\omega - \varepsilon}{\omega^2} \tag{21}$$
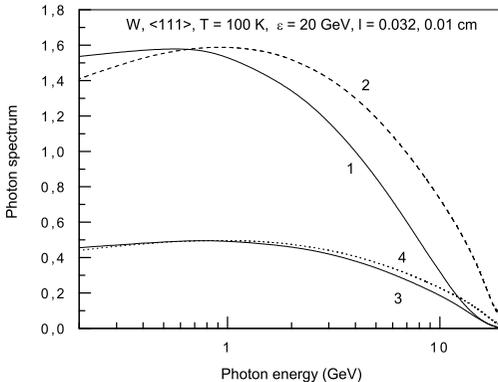
This formula has the same structure as Eq.(20).

9

Fig. 2. The spectral distribution of radiation at the initial electron energy $\varepsilon_0 = 20$ GeV in the tungsten crystal, axis $< 111 >$, T=100 K in two targets with thickness $l = 0.032$ cm$= 0.77\ L = 0.16\ L_{pr}$ (curves 1 and 2) and $l = 0.01$ cm$= 0.24\ L = 0.093\ L_{pr}$ (curves 3 and 4) vs the photon energy ω. The curves 2 and 4 are calculated according to Eq.(8), while the curves 1 and 3 are calculated according to Eq.(13) which takes into account the electron energy loss.

In Fig.2 the spectral distribution of radiation $\omega dn_\gamma^{(in)}/d\omega$ is shown. The final electron energies are correspondingly $\varepsilon_l = 10$ GeV and $\varepsilon_l = 16$ GeV for the used thicknesses. It is seen that at $\omega > 16$ GeV the curves 2 and 4 merge. For $\varepsilon_0 - \omega \ll 5$ GeV the spectral distribution is in a good agreement with Eq.(15)(without the factor $\exp(-W(\varepsilon_0)l)$) (at $\omega > 19$ GeV it is better than 5%). This factor, considering the photon absorption with the energy $\omega \simeq \varepsilon_0$ when photon is crossing the whole crystal, is 0.85 and 0.91 for the used thicknesses. The curve 2 and 4 calculated for thin targets differ only on a scale (ratio of their ordinates coincides with the ratio of thicknesses). In the soft part of spectrum the difference between the curves 1 and 2 is not very large. It is in agreement with Eq.(16). This property of spectra in oriented crystals was indicated in [4]. In the hard part of spectrum the difference is quite essential and one has to take into account the energy loss in the case where the crystal thickness $l \simeq L(\varepsilon)$. In the case $l \ll L(\varepsilon)$ the essential distortion of the spectral curve occurs in the hard end of spectrum only as it is seen from comparison of the curves 3 and 4.

In Fig.3 the spectral distribution of radiation $\omega dn_\gamma^{(in)}/d\omega$ is shown. These parameters are used in the experiment NA63 carried out recently at SPS at CERN (for proposal see [6]). The final electron energies are correspondingly
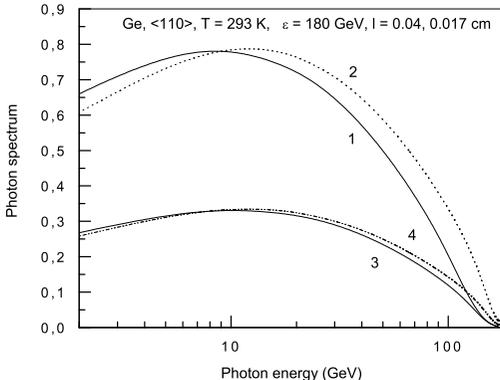
Fig. 3. The spectral distribution of radiation at the electron with energy $\varepsilon_0 = 180$ GeV in germanium crystal, axis $< 110 >$, T=293 K in two targets with thickness $l = 0.04$ cm= 0.38 $L = 0.064$ L_{pr} (curves 1 and 2) and $l = 0.017$ cm= 0.16 $L = 0.027$ L_{pr} (curves 3 and 4) vs the photon energy ω. The curves 2 and 4 are calculated according to Eq.(8), while the curves 1 and 3 are calculated according to Eq.(13) which takes into account the electron energy loss.

$\varepsilon_l = 124$ GeV and $\varepsilon_l = 153$ GeV for the used thicknesses. It is seen that at $\omega > 150$ GeV the curves 2 and 4 merge. For $\varepsilon_0 - \omega \ll 60$ GeV the spectral distribution is in a good agreement with Eq.(15)(without the factor $\exp(-W(\varepsilon_0)l)$) (at $\omega > 170$ GeV it is better than 8%). This factor, considering the photon absorption with the energy $\omega \simeq \varepsilon_0$ when photon crossing the whole crystal, is 0.94 and 0.97 for the used thicknesses. The curve 2 and 4 calculated for thin targets differ only on a scale (ratio of their ordinates coincides with the ratio of thicknesses). In the soft part of spectrum the difference between the curves 1 and 2 is not very large. It is in agreement with Eq.(16). In the hard part of spectrum the difference is quite essential and one has to take into account the energy loss in the case where the crystal thickness $l \simeq L(\varepsilon)$. In the case $l \ll L(\varepsilon)$ the essential distortion of the spectral curve occurs in the hard end of spectrum only as it is seen from comparison of the curves 3 and 4.

In Fig.4 the spectral distribution of radiation $\omega dn_\gamma^{(out)}/d\omega$ in a quite thick target is shown. The final electron energy at the exit from the target is $\varepsilon_l = 8.1$ GeV. The factor, characterizing the additional suppression of the spectral distribution in the hard end, is $\exp(-W(\varepsilon_0)l)$=1/4.5. The quite substantial difference between the solid and dashed curves is connected with
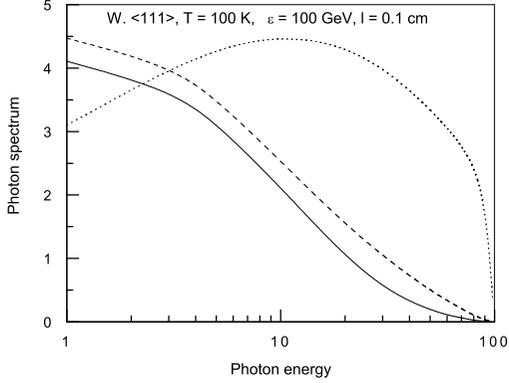
11

Fig. 4. The spectral distribution of radiation at the electron initial energy $\varepsilon_0 = 100$ GeV in the tungsten crystal, axis $< 111 >$, T=100 K in the target with thickness $l = 0.1$ cm= 3.15 $L(\varepsilon_0) = 1.505$ $L_{pr}(\varepsilon_0)$. The dotted curve is calculated according to Eq.(8), the dashed curve is calculated according to Eq.(13) which takes into account the electron energy loss and the solid curve is calculated according to Eq.(14) which takes into account both the electron energy loss and the photon absorption
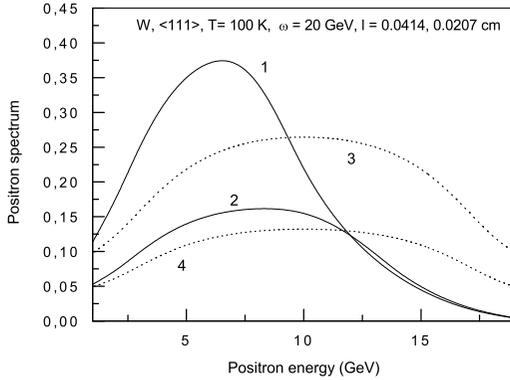

Fig. 5. Spectra of positrons created by the photon with energy $\omega = 20$ GeV in the tungsten crystals (axis $< 111 >$, T=100 K) with thickness $l = 0,0414$ cm=$L(\omega)$ and $l = 0,0207$ cm=$L(\omega)/2$. The curves 3 and 4 are calculated for thin targets according to Eq.(1), while the curves 1 and 2 are calculated according to Eq.(20) which takes into account both the positron energy loss and the photon absorption

12

the relatively large number of e^+e^- pairs created by radiated photons. The particles of these pairs emit photons also. However, a consideration of the next stage of cascade is out of scope this paper.

In Fig.5 the distortion of the positron spectrum is shown due to the photon emission from positrons and the initial photon absorption in a rather thick target. The curves 3 and 4 calculated for the thin target are symmetric with respect to point $\omega/2$=10 GeV. The area under the curves 1 and 2 divided by $\omega = 20$ GeV give the total number of created pairs in the interval from 1 to 19 GeV's. Since at calculation of the curves 3 and 4 the photon absorption was not taken into account the area under these curves is by 10%(5%) larger than under the curves 1 and 2 respectively. The hard end of the curves 1 and 2 is in a good agreement with Eq.(21). According to this equation the difference between these curves is due to difference of the factors $\exp(-Wl)$ equal to 0.8 and 0.9 respectively.

3   Conclusion

In this paper the spectral distribution of particles of electron-positron pair created by a photon and the spectral distribution of radiation from an electron in an oriented crystal of the intermediate thickness $l \sim L(\varepsilon_0)$ is calculated for the energy $\varepsilon(\omega) \sim \varepsilon_m$. The theory approach is developed which takes into account the energy loss due to the photons emission from charged particles as well as the absorption of photons in a crystal. For the first time the closed analytical expressions were obtained for description of the starting stage of the electron-photon cascade in oriented crystal. Since in the energy region under consideration all the specific mechanisms (coherent and incoherent radiation(pair creation), the LPM-effect) are essential, we used the recently developed method which includes all these mechanisms (see Eqs.(1), (8)). It turn out to be important at the cascade analysis that for the energies and thicknesses under consideration the probability of secondary processes is suppressed because of the relatively large photon absorption length $L_{pr}(\omega \sim \varepsilon_m) \gg L(\varepsilon \sim \varepsilon_m)$. Some estimates of the number of electrons and photons at the exit of target are given Sec.20.4 [5], where one can found also the results of simulation of experimental data.

The results obtained show the substantial variation of the hard photon spectral distribution comparing with thin target even for the relatively thin targets (see Figs.2,3). At the same time the deformation of the soft part of spectra is quite modest. The found positron energy distribution at $l \sim L(\varepsilon)$ demonstrates the dramatic difference from the spectrum in thin crystal. In

13

the relatively thick tungsten crystal $l \gg L(\varepsilon_0)$ (Fig.5) and at the high electron energy $\varepsilon_0 \gg \varepsilon_m$ we found the dramatic variation of the emitted photon spectrum comparing with thin crystal. In this case the appreciable number of secondary pairs are created and the next stages of cascade process should be studied.

Acknowledgments

References

[1] V.N. Baier, and V.M. Katkov, Phys. Lett., A 346 (2005) 359.

[2] V.N. Baier, and V.M. Katkov, Phys. Lett., A 353 (2006) 91.

[3] V.N. Baier, and V.M. Katkov, Phys. Lett., A 272 (2008) 2904.

[4] V.N. Baier, V.M. Katkov, Nucl. Instr. and Meth., B 266 (2008) 3828.

[5] V.N. Baier, V.M. Katkov and V.M. Strakhovenko, *Electromagnetic Processes at High Energies in Oriented Single Crystals*, World Scientific Publishing Co, Singapore, 1998.

[6] J.U. Andersen, K. Kirsebom, S.P. Moller *et al*, *Electromagnetic Processes in Strong Cristalline Fields*, CERN-SPSC-2005-030.

V.N. Baier and V.M. Katkov

**Spectra of radiation and created particles
at intermediate energy in oriented crystal
taking into account energy loss**

В.Н. Байер, В.М. Катков

**Спектры излучения и рождённых частиц
при промежуточных энергиях в ориентированных
кристаллах с учётом потери энергии**

Budker INP 2008-37